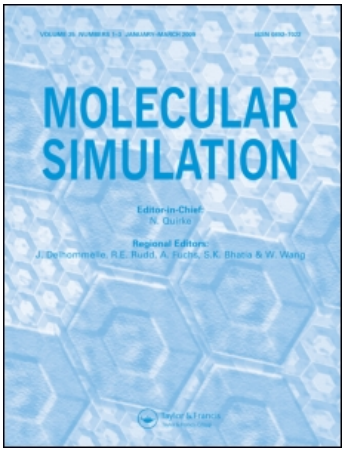

Molecular Simulation
Publication details, including instructions for authors and subscription information:
http://www.informaworld.com/smpp/title~content=t713644482

Condensed State Molecular Dynamics in Sorbitol and Maltitol: Mobility Gradients and Conformation Transitions

B. Sixou[a]; L. David[a]; M. M. Margulies[b]; J. Y. Cavaillé[a]; G. Vigier[a]
[a] Groupe d'Etudes de Métallurgie Physique et de Physique des Matériaux, Institut, National des Sciences Appliquées de Lyon, Villeurbanne Cedex, France [b] Laboratoire de Mecanique Physique, Universite Paris, Creteil Cedex, France

To cite this Article Sixou, B. , David, L. , Margulies, M. M. , Cavaillé, J. Y. and Vigier, G.(2001) 'Condensed State Molecular Dynamics in Sorbitol and Maltitol: Mobility Gradients and Conformation Transitions', Molecular Simulation, 27: 4, 243 — 265
To link to this Article: DOI: 10.1080/08927020108027950
URL: http://dx.doi.org/10.1080/08927020108027950

Molecular Simulation, 2001, Vol. 27, pp. 243–265
Reprints available directly from the publisher
Photocopying permitted by license only

CONDENSED STATE MOLECULAR DYNAMICS IN SORBITOL AND MALTITOL: MOBILITY GRADIENTS AND CONFORMATION TRANSITIONS

B. SIXOU[a,*], L. DAVID[a], M. M. MARGULIES[b], J. Y. CAVAILLÉ[a] and G. VIGIER[a]

[a]*Groupe d'Etudes de Métallurgie Physique et de Physique des Matériaux, Institut, National des Sciences Appliquées de Lyon, Bât. 502, 20 av. A. Einstein, 69621, Villeurbanne Cedex, France;* [b]*Laboratoire de Mecanique Physique, Universite Paris 12 Val de Marine, 61 avenue de, General de Gaulle, 94010 Creteil Cedex-France*

(Received November 2000; accepted January 2001)

Molecular mobility in sorbitol and maltitol is studied in order to understand their differences near the junction between the α and β relaxations. The molecular dynamics simulations performed on the polyols in their bulk state give support to the ^{13}C NMR results and imply that the mobility of a carbon atom located at the extremity of the chain is higher than that of any other carbon. Moreover, the difference in carbon atoms mobility is greater within the sorbitol moiety of maltitol than in sorbitol and seems intimately related to the junction temperature of the α and β relaxation processes. The reorientation of the C—H vectors as probed by NMR is shown to be mainly the effect of conformation transitions in the case of a carbon atom located at the end of the chain.

Keywords: Molecular mobility; Conformation transitions; Sorbitol; Maltitol

1. INTRODUCTION

Molecular moblity in polymers and glasses manifests itself through one universally observed relaxation phenomenon associated with the glassy

*Corresponding author. Fax: 33-0472438528, e-mail: bruno.sixou@insa-lyon.fr

transition (α relaxation) and through one or several secondary relaxation processes corresponding to local rearrangements (β and γ relaxations). Yet, one still ignores the precise nature of the molecular events responsible for theses relaxations and the atomic interpretation of cooperativity of these movements. The secondary β relaxation has been particularly studied in numerous glasses but the question of its origin remains open [1–4]. In this context, molecular dynamics and mechanics methods are expected to allow a rather precise identification and caracterization of the β movements and a detailed study of their statistical properties and of their relationships with local conformational changes [5–7].

In this article, we study two similar organic glass-formers, namely sorbitol and maltitol. Several authors have looked at the β relaxation and the $\alpha-\beta$ relaxation in sorbitol in detail [8–10]. They emphasize the fact that relaxation studies require homogeneous transparent samples. The relaxation diagram of sorbitol and maltitol, which displays the evolution of the characteristic relaxation times τ as a function of the reciprocal of the temperature (Fig. 1), has been obtained with different spectroscopic techniques: viscosity measurements, dielectric and mechanical spectroscopies,

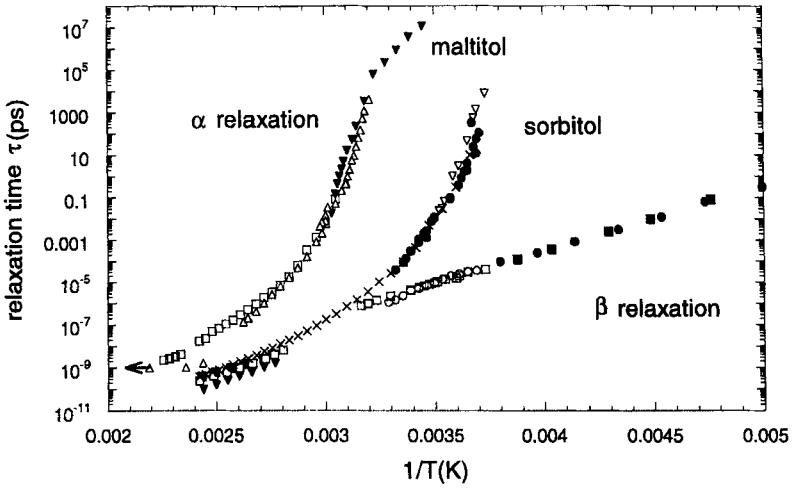

FIGURE 1 Relaxation diagram of sorbitol and maltitol [17]: α relaxation of maltitol, viscosity (□), dielectric spectroscopy (△), mechanical spectroscopy (▼); α relaxation of sorbitol, viscosity (×), dielectric spectroscopy (•), mechanical spectroscopy (▽); β relaxation of sorbitol, dielectric spectroscopy (□), mechanical spectroscopy (■); β relaxation of maltitol, dielectric spectroscopy (○), mechanical spectroscopy (•). Relaxation times obtained by means of ^{13}C NMR for carbon atoms C_4 (■), C_2(□) and C_1(▼) in sorbitol. Relaxation times obtained by means of ^{13}C NMR for carbon atoms C_4(▽) and C_1(△) in maltitol. The arrow means that the estimated temperature corresponds to a lower bound [17].

quasielastic neutron scattering [11, 12]. Two relaxations processes can be observed. The slower one, the α relaxation process, exhibits a non-Arrhenius behaviour above the glass-transition T_g. It follows the Vogel-Fulcher function given by $\log(\tau) = A - C/(T - T_0)$. The best fit is obtained with parameters $A = 12.25$, $C = 531\,K$, $T_0 = 233\,K$ and $A = 17.2$, $C = 164\,K$, $T_0 = 228\,K$ for sorbitol and maltitol respectively, which are very similar values to those reported in Refs. [8] and [10]. An Arrhenius behaviour is found for temperatures below T_g. An other secondary relaxation process (β process) appears at higher frequencies, with a linear behaviour *versus* $1/T$. As observed on the relaxation diagram, Figure 1, the β relaxation in sorbitol and maltitol occurs on the same time-temperature range and the relaxation times associated with this relaxation show an activated temperature dependence with the same apparent activation energy, $E_\beta \sim 60\,kJ/mole$, in agreement with the values reported in Refs. [8 – 10]. This result suggests that the β process could have the same molecular origin in both systems. On the contrary, sorbitol and maltitol display very different behaviours in the cross-over region between the α and β relaxation. As reported in Refs. [8 – 10], this cross-over occurs between 290 and 335 K for sorbitol and could not be observed for maltitol in the temperature range studied. It is likely that this relaxational behaviour difference can be ascribed to the glucopyranosyl moiety present at the centre of the chain in maltitol. One may consider that the temperature $T_{\alpha\beta}$ corresponds to the temperature for which global motions becomes as fast as local motions. In the framework of this assumption, fast global and cooperative motions and the crossover between the two relaxation processes occurs for higher temperatures in maltitol because of the more complex molecular structure and of the hindrance induced by the glucopyranosyl cycle. The ratio $T_{\alpha\beta}/T_g$ is 1.2 for sorbitol, in agreement with a few values observed in some fragile liquids [13]. Very little information is given in the literature about the cross-over between these relaxations because it is difficult to separate the contributions of the two processes in the temperature-frequency window where they meet [14]. Goldstein and Johari suggested that the β relaxation is an intrinsic property of the glassy state, due to local rearrangements. This interpretation leads to a tangential merging of the α and β processes at high temperature [15]. Our results show that, if for maltitol this assumption could be valid, for sorbitol, the linear extrapolation of the β process clearly crosses the α relaxation process. A clear crossover is observed in other polymers systems like polystyrene or PMMA. More recently, Rössler proposed that the bifurcation between both processes happens at a temperature $T_{\alpha\beta}/T_g = 1.18 - 1.28$ [13], $T_{\alpha\beta}$ being close to the critical temperature T_c of the Mode Coupling Theory

[16]. This result can account for the relaxational behaviour of the sorbitol molecule but is not in agreement with the one of maltitol.

In order to consider these issues, we thus present ^{13}C NMR measurements of the correlation times of the molecular motions related to the C—H bonds together with molecular dynamics simulations, based on an atomic description of the systems. The information coming from the simulations, which create a link between the atomic structure of the polyols and their microscopic properties, especially their dynamic behaviour and the molecular mobility of the various atoms, are expected to be in agreement with the NMR results, which allow to study separately the mobilities of the various carbon atoms on the main chain. In a previous paper, we have compared in detail the local chain dynamics in isolated sorbitol and maltitol as determined from molecular dynamics simulation with results of experimental ^{13}C NMR studies [17]. It was shown that the mobility of carbons located at the end of the 6 carbon chain is greater than that of any other carbon of this chain and it was suggested that the merging difference between the α and β relaxation processes in both sugars would be related to the mobility differences between the atoms of the main chain. In the present work, we study the dynamic properties of sorbitol and maltitol by considering in detail their molecular motions in the molten liquid state. It is worth mentioning that molecular dynamics simulations can describe processes with a time scale of the order of the nanosecond. Thus the comparaison between the relaxation diagram and the results of the simulation is restricted to the low left corner of the relaxation diagram. Yet, we hope that the limited time /temperature range investigated can give interesting informations related to the relaxational processes occuring on longer time scales. We first present the simulations methods and summarize the NMR results. Then, we detail the relaxational behaviour of sorbitol and maltitol molecules as determined from the molecular dynamics simulations. As part of the discussion, we consider the relation between the intramolecular mobility gradients and the α and β relaxations crossover together with the connection of local chain dynamics to conformational transitions.

2. EXPERIMENTAL

2.1. Materials

The chemical structure of D-sorbitol and maltitol (4-O-α-D-glucopyranosyl-D-sorbitol) are displayed in Figure 2. D-sorbitol of 99% purity was

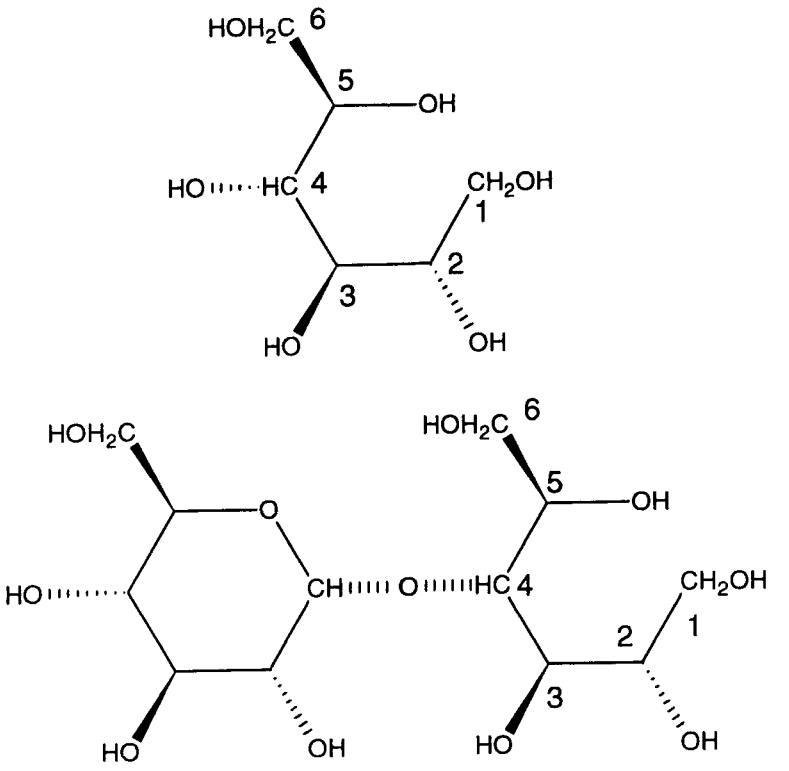

FIGURE 2 Chemical structure of maltitol and sorbitol and numbering of their carbons.

purchased form Merck (reference 7759) and maltitol of 99% purity was given by Roquette Freres (France). After heating well above the melting temperature T_m ($T_m = 453\,K$ for maltitol and $T_m = 420\,K$ for sorbitol respectively), the samples were cooled to room temperature under argon atmosphere. The samples obtained are transparent. All measurements were reversible in temperature showing that no detectable crystallization takes place. The glass transition temperatures of these molecular systems are respectively $T_g = 273\,K$ for sorbitol and $T_g = 323\,K$ for maltitol, as measured by DSC with a heating rate of 3 K/min [11–12]. The higher value of T_g for maltitol can be related to the more complex structure of this polyol. For convenience, the carbon atoms and torsion angles have been numbered along the chain. We refer to the carbon atom and to the torsion angle at the end of the chain as C_1 and a_1 ($0—C_1—C_2—C_3$) and to the ones located in the middle of the chain as C_4 and a_3 ($C_2—C_3—C_4—C_5$). Torsion angles are defined as in the literature [18].

2.2. Force Field and Simulation Methodology

In this section, we present details of the simulations performed on the bulk sorbitol and maltitol molecules submitted to periodic boundary conditions. The molecular mechanics and molecular dynamics simulations were performed using CVFF95 force field as integrated in the Cerius program (Molecular Simulation Inc., San Diego, California, USA). This force field is devised for organic polymers and small organic molecules and described in detail elsewhere [19–24]. The potential energy was described as the sum of bond stretch, angle bending, torsional, van der Waals and electrostatic terms. The nonbonded interactions are represented by a Lennard-Jones 12-6 potential. In the CVFF force field, hydrogen bonds are a natural consequence of the standard VDW and electrostatic parameters, and special hydrogen bond function do to improve the fit of CVFF to experimental data [19–24]. The bulk structure of sorbitol and maltitol was simulated with cubic periodic boundary conditions and minimum image convention, a method which has been successfully used to simulate bulk polymers and polymers melts [25]. In a first step, since the starting structure may influence the simulation results, three amorphous structures with different conformational properties were generated by using the Monte Carlo method for dihedral angles of all rotatable backbone bonds as implemented in the Amorphous Builder modulus of Cerius. During this generation process, the chain grows in the cell bond by bond and if it passes through one face of the cell, it would reenter through the opposite face. If the distance of two non bonded atoms is smaller than the sum of their atomic radii, the corresponding conformation is rejected. To enhance the efficiency, the Van der Waals radii of all atoms were reduced to 30% of their actual values during the whole growing process. In order to ensure the convergence of the growing process, the density of bulk sorbitol and maltitol were set respectively at 1.34 and 1.49 g/cm^3, which are slightly lower than the cristalline sorbitol and maltitol densities (1.489 and 1.61 g/cm^3). The initial structures obtained have very high potential energy as a result of the crude growing process. The relaxation of these high-energy structures was handled with care. A simple molecular mechanics energy minimization will lead the system to the nearest local minimum, which has still a high potential energy. Therefore, in the literature great efforts were made to get a relative low-energy conformation of such systems [26–29]. For this step, we choosed a strategy similar to the one used by Mattice *et al.* [28, 29]. Hundred picoseconds NVT molecular dynamics runs are successively performed at 300 K, 400 K, 500 K and 600 K. The initial structure of each run is the

conformation with the lowest total potential energy during the proceeding simulation which has been selected and whose potential energy has been minimized using the steepest descent method. The last step consists in obtaining stable potential energy and density, with runs of a few nanosecondes in the constant stress and temperature (NST) statistical ensemble and for temperatures ranging between 350 and 600 K The overall potential energy of the structures obtained remains stable and is significantly lower than the one of the initial molecules. This energy difference was estimated to 10 kJ/mole. Moreover, the components of the internal stress tensor of the relaxed structures, which can be easily calculated [29], are smaller than 0.025 GPa. At last, we have obtained small differences of total energy among the three structures generated. This relaxation strategy is thus able to bring the initial structures to a reasonable low-energy state. At the end of the whole relaxation process and for both polyols, we have used the three structures generated for 1 ns molecular dynamics runs carried out in the NST statistical ensemble for subsequent analysis. At the end of each simulation, 1000 conformations were recorded. The temperatures chosen for these simulations were 350 K, 370 K, 400 K, 420 K, 450 K and 500 K and the pressure was held constant at 1 bar. Simulations were performed using the weak coupling scheme to a temperature or pressure bath [25, 30]. The equation of motion were solved with the Verlet algorithm with a time step of 1 fs. All the results presented in the following for both polyols are the averages calculated with the simulations performed with the three relaxed structures.

3. ^{13}C NMR RESULTS

The NMR measurements performed on sorbitol and maltitol in their liquid state have been detailed elsewhere [17]. The main interest of the NMR technique is that the mobility of each carbon atom of the considered molecules can be investigated separately by means of spin-lattice relaxation time measurements.

3.1. Principle of the Analysis of the NMR Measurements

Considering the dipolar interactions between the magnetic moments of the protons attached to the polymer chain, and if the dynamics of the molecular process observed from NMR is governed by a single correlation time

$\tau_{NMR}(T)$, the spin-lattice relaxation time, T_1, verifies [31]:

$$\omega_0/T_1(\omega_0, T) = f(\omega_0 \times \tau_{NMR}(T)) \quad (1)$$

where ω_0 is the Larmor angular frequency, T the temperature, and f a function of the Larmor frequency and of the temperature, exclusively through the $\omega_0 \cdot \tau_{NMR}(T)$ product. This result is also valid if all correlation times of the correlation time spectrum have the same type of temperature dependence and are proportional to a single basic correlation time, as it is the case for the Rouse spectrum for example. The temperature dependence of τ_{NMR} can be determined by measuring the temperature dependence of the spin-lattice relaxation time T_1 at two distinct Larmor frequencies ($\omega_0 = 62.9$ MHz and 101 MHz). Details on this step by step procedure used are given in references [17] and [31–34]. In order to use formula (1), we assume that:

(i) the correlation times calculated are associated to a single relaxation process, α or β depending on the C atom considered, if these processes are well separated in the temperature range studied.
(ii) when this is not the case, in the vicinity of the junction temperature $T_{\alpha\beta}$, T_1 is determined by both the α and β processes, but their characteristic time scales can be approximated by Arrhenius dependences with similar activation energies but different prefactors, and formula (1) is still valid.

3.2. Results of the ^{13}C NMR Experiments for the Sorbitol and Maltitol Molecules

Selected results of the NMR study are summarized in this section. The temperature dependences of the correlation times derived from the NMR measurement are displayed in Figure 3 for the various carbon atoms of sorbitol and maltitol. They have been obtained on a small temperature range because of the Larmor frequencies used. In the case of the sorbitol molecule, the logarithm of τ_{NMR} is a linear function of the reciprocal of the temperature, T, for all carbon atoms in the relatively short temperature range investigated (Fig. 3). We have thus fitted this temperature variation by the following Arrhenian law:

$$\tau_{NMR}(T) = \tau_{0,NMR} \exp(E_{NMR}/RT)$$

The activation energy E_{NMR} and the preexponential time $\tau_{0,NMR}$ determined are given in Table I for the various carbon atoms of sorbitol.

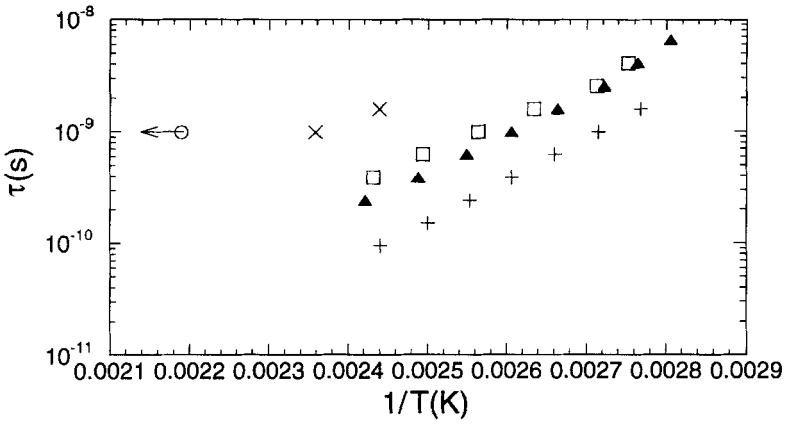

FIGURE 3 Temperature dependences of the relaxation times obtained by means of ^{13}C-NMR, for carbons C_4 (□) C2 (▲) and C_1 (+) in sorbitol; relaxation times obtained by means of ^{13}C NMR for carbon atoms C_4(o) and C_1(×) in maltitol.

TABLE I Activation energies E_{NMR} and preexponential factors $\tau_{0,NMR}$ obtained for sorbitol carbons with the NMR measurements

Carbons	E_{NMR} *(kJ/mol)*	$\tau_{0,NMR}$ *(s)*
C_4	65 ± 7	$2\ 10^{-17}$
C_2		$3\ 10^{-19}$
C_1		$6\ 10^{-20}$

As detailed in reference [17], the ^{13}C NMR results show that:

- the mobility of a carbon atom located at the end of the molecule (C_1) is greater than that of a carbon located in the center of the molecule (C_4) ($\tau(C_4-H)/\tau(C_1-H) \approx 3$ in sorbitol).
- the difference in carbon mobility is greater within the sorbitol moiety of maltitol than in sorbitol, a result that may be related to the rigidity associated with the glycosidic chemical bond between the main chain and the glucopyranosyl cycle in maltitol.

Moreover, the activation energy deduced for each sorbitol carbon-atom (65 ± 7 kJ/mole) is close to the β relaxation activation energy of the whole molecule of sorbitol or maltitol obtained in the low temperature range ($E\beta \sim 60$ kJ/mole [11, 12]). It is also close to the activation energy E_α deduced from a fitting of the α relaxation process by an Arrhenius law in the temperature range near 400 K ($E_\alpha \sim 70$ kJ/mole). More precisely, it was suggested that the correlation times of the carbon atom C_4 and C_1 are

intimately related to the time scales of the $\alpha(\tau_\alpha)$ and $\beta(\tau_\beta)$ relaxation processes respectively [17]. We have also proposed that the crossover between the α and β relaxations in sorbitol and maltitol may be related to the mobility difference of C_1 and C_4 carbon atoms at a given temperature. A merging at high temperature, as observed in maltitol, being concomittant with large mobility differences, and reciprocally, a crossover at lower temperatures and longer times, as found in sorbitol, should be associated with a more homogeneous mobility of the carbon atoms of the molecule.

4. MOLECULAR DYNAMICS SIMULATIONS RESULTS

The molecular dynamics simulations results presented in the following are the averages obtained from the runs performed on the three relaxed structures of each polyol. The analysis of the results consists in the calculation of characteristic correlation times and of conformation transition rates.

4.1. Correlation Times and Conformation Transition Rates

4.1.1. Reorientation of Bond Vectors

From the molecular dynamics simulations, we have tried to extract several correlation times to be compared with the characteristic times scales obtained from the NMR results. The T_1 values measured by ^{13}C NMR are sensitive to the reorientation of the C—H bonds. The correlation time obtained from a ^{13}C NMR T_1 spin-lattice relaxation time depends on the orientation autocorrelation function $P_2(t)$ for a unit vector X(t) pointing in the direction of a particular C—H bond vector at time t [31]:

$$P_2(t) = \langle LP_2(\mathbf{X}(0) \cdot \mathbf{X}(t))\rangle = \langle 3\cos^2\theta(t) - 1\rangle/2$$

Where LP_2 is the second Legendre polynomial and $\theta(t)$ is the change in the vector orientation between time t and time 0. The brackets in this expression means an ensemble average. These calculation has been performed for a carbon atom at the end of the chain, *i.e.*, for the carbon atom C_1, and for a carbon atom at the middle of the chain C_4, for both polyols and for each simulation temperature.

4.1.2. Conformational Transitions Rates and Torsional Relaxation

The conformational state for a torsion angle can be defined from its potential energy curve, or from the actual dihedral distribution obtained

from the simulation. The distribution method represents the actual population of different torsion angles in the simulation. A stable conformational state corresponds to a maximum on the distribution curve. The population minimum between the two adjacent states defines a transition state. A conformational transition from an initial state to a final state is realized if a dihedral rotation crosses the boundary between the two states [35]. As an example, Figure 4 depicts the calculated distribution of the torsion angle a_1, which involves the four atoms $0—C_1—C_2—C_3$ at the extremity of the six carbon atom chain, at $T = 500\,K$, for the bulk sorbitol molecule. Arbitrary scales are used in the vertical axis. We have evaluated the average number of conformational transitions per nanosecond, N, for each torsion angle along the six carbon atom chain and the inverse of the transition rate, 1/N, which is the average time separating two successive transitions. The local motions are also discussed by looking at torsional relaxation of backbone bonds. A second-order time autocorrelation function can be defined for the dihedral a_i as:

$$G_2(t) = \langle 3\cos^2(a_i(t) - a_i(0)) - 1\rangle/2$$

which characterize the overall rotational diffusion process [36].

4.2. Results of the Molecular Dynamics Simulations

4.2.1. Reorientation of Bond Vectors

Figure 5 shows in a semi-logarithmic plot the evolutions of the correlation functions $P_2(t)$ for the $C_1—H$ and $C_4—H$ bonds vectors in bulk sorbitol at

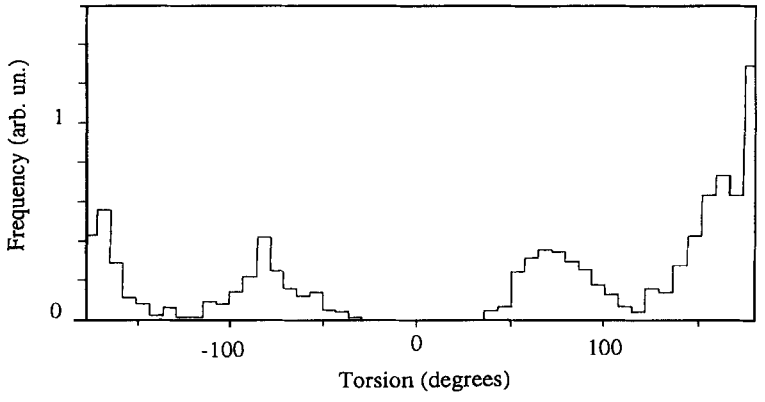

FIGURE 4 Distribution of the torsion angle a_1 at $T = 500\,K$ for the bulk sorbitol molecule obtained from the simulation.

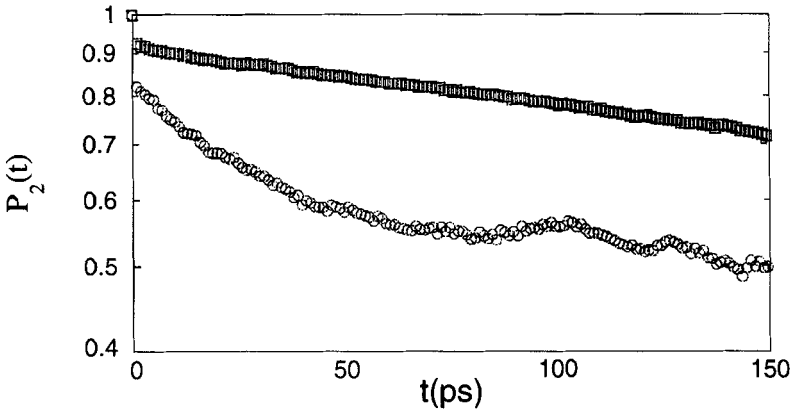

FIGURE 5 Semi-logarithmic plot of the relaxation functions P_2 *versus* time at T = 400 K in sorbitol, for the C_1—H(o) and C_4—H (□) bonds vectors in the bulk state.

T = 400 K. For convenience, the $P_2(t)$ evolutions of one of the relaxed initial structures have been arbitrarily selected for this plot. These curves diplays a very fast decrease during the first picosecond, and then a slower decrease. If one neglect the molecular motion of the first picosecondes which can be ascribed to librations, the decrease of the logarithm of the functions P_2 as a function of the time can be considered as linear. This result indicates that the P_2 correlation functions can be fitted by a single exponential and that the C—H bond vectors lose their orientation on a single relaxation timescale τ derived from the initial slope of the former plot:

$$P_2(t) = \exp(-t/\tau) \tag{2}$$

The P_2 decay were also fitted to the Kolrausch-Williams-Watts function:

$$P_2(t) = \exp(-(t/\tau)^{\beta}) \tag{3}$$

Yet, the β parameters found are close to the value $\beta = 1$ ($\beta = 0.95 \pm 0.3$) and no trend as a function of temperature can be clearly evidenced. The average values of the correlation times obtained for the sorbitol molecule in the bulk state are summarized in the Table II. They have been numbered like the

TABLE II Calculated correlation times for the reorientation of the C_1—H and C_4—H bond vectors for the bulk sorbitol molecule as a function of the temperature

T(K)	350	370	400	420	450	500
τ_1 (ps)	2000	350	245	155	80	35
τ_4 (ps)	–	8280	1500	1075	600	180

carbon atoms, τ_1 refers to C_1 and τ_4 to C_4. At 350 K, the correlation time τ_4 is too high to be evaluated with accuracy. The temperature dependences of the correlation times obtained for bulk sorbitol are displayed on Figure 6 together with the NMR results. A similar study has been performed on the maltitol molecule. The ^{13}C NMR study of this polyol is less comprehensive [17] and thus the comparison with the molecular dynamics simulations is more difficult. The evolution of the correlation time τ *versus* temperature is summarized in Table III and displayed on Figure 7 together with the two experimental points associated with the carbon atom C_1 and C_4, which have been determined with ^{13}C NMR measurements. Again, the temperature dependences of the correlation times can be accounted for by an Arrhenius law on the whole temperature range investigated:

$$\tau = \tau_0 \exp(\Delta E/RT) \tag{3}$$

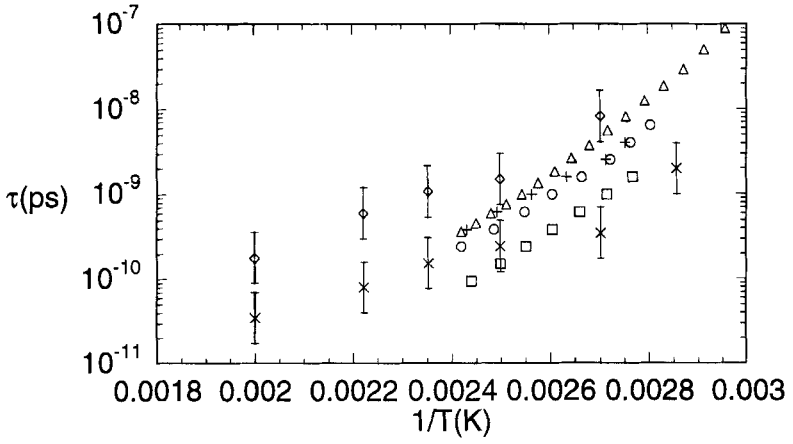

FIGURE 6 Temperature dependences of sorbitol relaxation times obtained from the ^{13}C NMR measurements for the C_1—H (□), C_2—H (o) and C_4—H (+) bond vectors; molecular dynamics simulations results for the C_1—H (×) and C_4—H (◇) bonds vectors in the bulk state; the α relaxation of sorbitol (Δ) is also displayed for comparison.

TABLE III Calculated correlation times for the reorientation of the C_1—H and C_4—H bond vectors for the bulk maltitol molecule as a function of the temperature

T(K)	350	400	420	450	500
τ_1(ps)	3700	1680	680	425	105
τ_4(ps)	–	28500	18000	3200	625

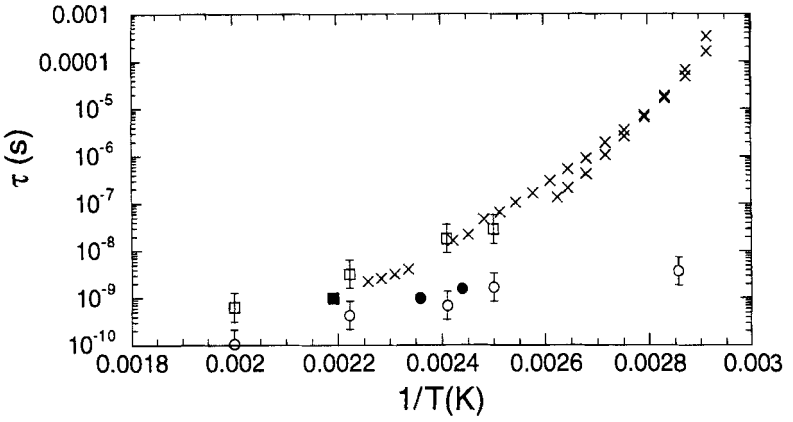

FIGURE 7 Temperature dependences of the maltitol relaxation times: (×) α relaxation; ^{13}C NMR results for the C_1—H (•) and C_4—H (■) bond vector; molecular dynamics simulation results for the C_1—H (o) and C_4—H (□) bonds vectors in the bulk state.

Where ΔE is the molecular activation energy and τ_0 the preexponential time. The values of the activation energies and of the preexponential times obtained for bulk sorbitol and maltitol molecules are summarized in Table IV and V respectively.

4.2.2. Torsional Relaxation and Conformation Transitions Rates

Figure 8 displays in a semi-logarithmic plot the time evolution of the second-order correlation function $G_2(t)$ for the dihedrals a_1 and a_3 at T = 400 K for a selected sorbitol structure. A fast decrease is again observed

TABLE IV Calculated activation energies and preexponential time obtained for the carbon atom C_1 and C_4 of the sorbitol molecule in the bulk state

Carbon atom	C_1	C_4
τ_0(ps)	6.510^{-3}	5.910^{-3}
ΔE(kJ/mol)	35	42.5

TABLE V Calculated activation energies and preexponential time obtained for the carbon atom C_1 and C_4 of the maltitol molecule in the bulk state

Carbon atom	C_1	C_4
τ_0(ps)	3.610^{-2}	9.510^{-5}
ΔE(kJ/mol)	34	65

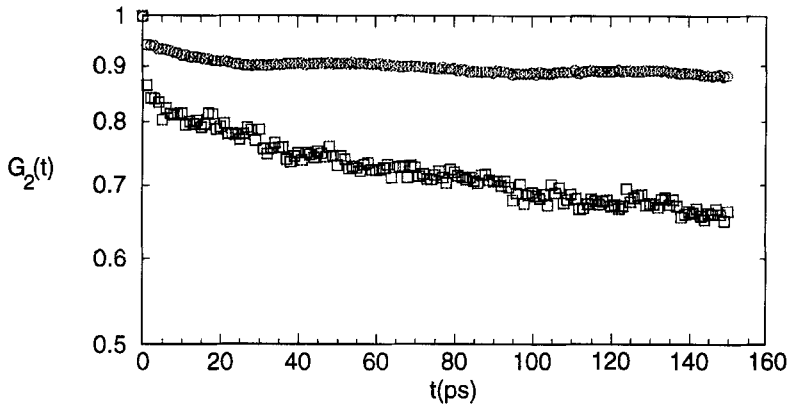

FIGURE 8 Semi-logarithmic plot of the relaxation functions G_2 *versus* time at T = 400 K in sorbitol, for the dihedral a_1(□) and a_3(o) in the bulk state.

during the first picoseconds, which can be ascribed to oscillations within a single rotational potential energy well [36]. For longer time scales, the $G_2(t)$ functions were approximated by the simple exponential:

$$G_2(t) = \exp(-t/\tau_\phi)$$

The time scale $\tau\phi$ was estimated for each temperature, for sorbitol and maltitol and for the dihedrals a_1 and a_3. The values obtained are listed in Table VI.

The inverses of the conformational transitions rates, $1/N_1$, obtained for the torsion angle a_1 of the bulk sorbitol and maltitol molecules are given in Table VII. In both polyols, in the case of the torsion angle in the middle of the chain, a_3, the number of conformation transitions N_3 is two low to be evaluated and therefore, a lower bound can be estimated for $1/N_3$:

$$1/N_3 \geq 1 \text{ ns}$$

TABLE VI Calculated torsional correlation times for the bulk sorbitol and maltitol molecule as a function of the temperature for the dihedrals a_1 and a_3

a) sorbitol						
T(K)	350	370	400	420	450	500
$\tau_{\phi 1}$(ps)	2980	518	384	226	120	45.5
$\tau_{\phi 3}$(ps)	–	–	2430	1270	936	266
b) maltitol						
T(K)	350	400	420	450	500	
$\tau_{\phi 1}$(ps)	6020	2520	950	680	154	
$\tau_{\phi 3}$(ps)	–	–	–	4830	850	

TABLE VII Number of conformation transitions during one nanoseconde obtained in condensed phase for the torsion angle a_1 in sorbitol and maltitol

T(K)	370	400	420	450	500
maltitol	–	–	1	3	5
sorbitol	2	4	5	7	25

Figures 9 and 10 display on a single plot the temperature dependences of $1/N_1$ and $\tau_{\phi 1}$ corresponding to the torsion angle a_1, and of the correlation time, τ_1, corresponding to the bond vector C_1—H obtained in bulk sorbitol and maltitol.

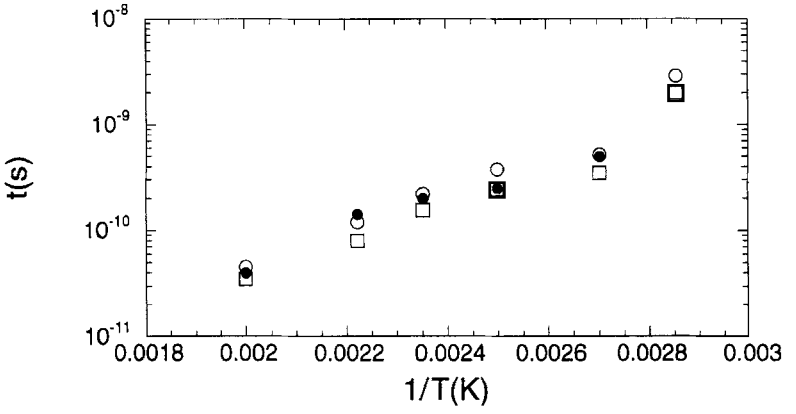

FIGURE 9 Temperature dependences of $1/N_1$(•), of the correlation time $\tau_{\phi 1}$ of the torsion angle a_1(o) and of the correlation time, τ_1(□), of the bond vector C_1—H obtained in bulk sorbitol.

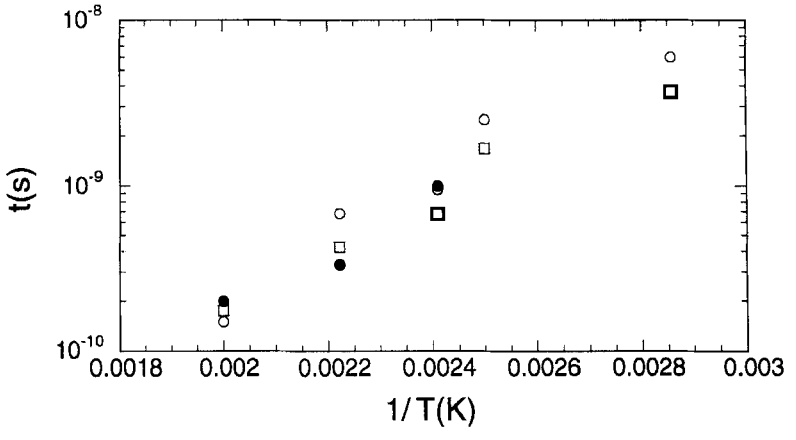

FIGURE 10 Temperature dependences of $1/N_1$(•), of the correlation time $\tau_{\phi 1}$ of the torsion angle a_1(o) and of the correlation time, τ_1(□), of the bond vector C_1—H obtained in bulk maltitol.

5. DISCUSSION

5.1. Comparison of the NMR Results with the Molecular Dynamics Simulation Results

We now detail the comparison of the correlation times obtained from the ^{13}C NMR and from the molecular dynamics simulations performed in condensed phase. The simulations qualitatively reproduce several important experimental results. The first point is the rather good agreement between the ^{13}C NMR and molecular dynamics simulation results. In the case of bulk sorbitol, Figure 6 shows that the correlation times obtained with the molecular dynamics simulations for the C_1 and C_4 atoms are of the same order of magnitude than the time scales derived from the NMR measurements. The same result is true for the C_1 carbon atom of bulk maltitol, for which few NMR data are available (Fig. 7). In all cases, the best agreement is obtained for the C_1 carbon atoms. The times scales obtained from the molecular dynamics simulations for the C_4 carbon atom of sorbitol are slightly shifted upwards as compared to the corresponding NMR data. As shown in Table IV and V, the activation energies obtained from the simulations on the bulk sorbitol and maltitol molecules are rather close to the ones obtained from the NMR experiments (65 kJ/mole). The more significant discrepancy between the ^{13}C NMR and molecular dynamics results is related to the preexponential times. All these results suggest, on the one hand, that the force field used is correct to describe our polyols and, on the other hand, that, on a certain extent, the few relaxed initial conformations obtained are representative of the dynamical properties of the bulk polyols. The second point of interest is that, as shown in Figures 6 and 7, the simulations confirm that the relaxation process of a carbon atom at the end of the chain is faster than the one of a carbon atom in the middle of the chain. The mobility gradient along the main chain, evidenced by the ^{13}C NMR results, is thus well reproduced by the simulations on both polyols. The third point was already suggested in Ref. [17] and is related to the former conclusion. As shown on Figures 6 and 7, the correlation times of a carbon atom at the middle of the chain, τ_4, and at the extremity of the chain, τ_1, are close to the relaxation times associated to the α and β relaxation processes respectively. In the case of maltitol, the two relaxation processes have not merged in the investigated temperature-frequency window. The extrapolated dielectric spectroscopy data obtained at lower temperatures for the β relaxation converge towards τ_1. In the case of sorbitol, the extrapolated data obtained at low temperatures for the β relaxation may converge towards the C_1 relaxation times, if only the highest temperature dielectric measurements are taken into account [17]. To a

certain extent, the mobility gradient can be interpreted as the characteristic time scales difference between the α and β relaxation process. In the framework of this assumption, τ_1 and τ_β should be associated to local motions and τ_4 and τ_α to more global motions. It must be emphasized that the data which corresponds to what is referred to as α relaxation have been obtained with viscosity measurements and after a normalisation treatment, which aims at combining informations issued from different techniques. The correct calculation of the correlation time associated to the α and β processes is still an open question since the extrapolation of the low temperature data of Figure 1 to the NMR measurements must be careful in view of the small temperature range investigated with NMR [17]. The qualitative agreement between the τ_4 and τ_α and τ_1 and τ_β times scales should therefore be considered with care. But, it enables us to propose an interpretation of the differences between the maltitol and sorbitol relaxational behaviours, as detailed in the following sections.

5.2. Comparison Between the Maltitol and Sorbitol Relaxation Behaviours

In order to compare the relaxational behaviours of bulk sorbitol and maltitol, Figure 11 displays on the same plot the temperature dependence of the relaxation times of the two polyols obtained from the simulations. The relaxation process is slower in maltitol on the whole temperature range. This

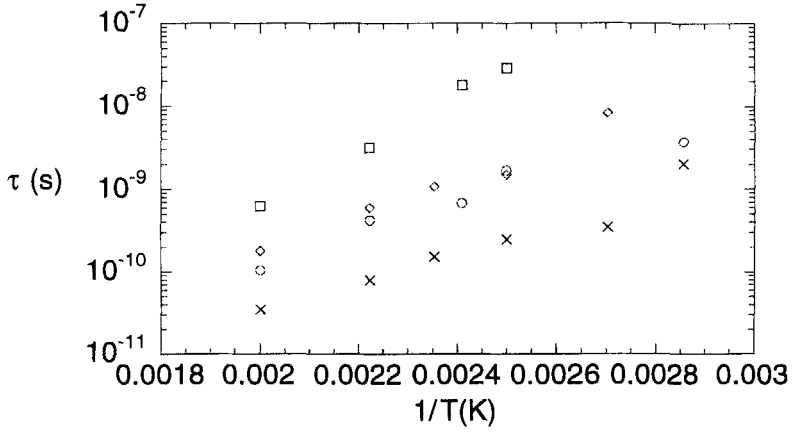

FIGURE 11 Temperature dependence of the relaxation times obtained from the simulations in bulk maltitol for the C_1—H(o) and C_4—H(□) bonds vectors and in bulk sorbitol for the C_1—H (×) and C_4—H (◇) bonds vectors.

conclusion is in agreement with the NMR results and may be interpreted as the effect of the more complex molecular structure of maltitol. It is also supported by the torsional correlation times and transition rates calculated (Tab. VI and VII). On the basis of the molecular dynamics simulations, we have evaluated the mobility gradients in maltitol and sorbitol by means of the ratio τ_1/τ_4 of the relaxation time of the carbon atoms located at the end of the main chain to the one of the atoms in the middle of this chain. The results are summarized in Table VIII. Two points are worth mentioning:

- in both polyols, the ratio τ_4/τ_1 seems to be a decreasing function of the temperature. This result could be related to the decrease with temperature of the ratio τ_α/τ_β of the characteristic time scales of the α and β relaxation process;
- the ratio τ_4/τ_1 and the mobility gradients are found higher in maltitol than in sorbitol, which is in agreement with the NMR results. If one assumes that τ_4/τ_1 is intimately related to the ratio τ_α/τ_β, these mobility gradients differences may be interpreted as the origin of the differences of relaxational behaviour at the junction between the α and β relaxations observed in two polyols. In the framework of this hypothesis, the higher junction temperature found in maltitol is the result of a higher molecular mobility gradient between the carbon atoms located at the end (C_1) or in the middle (C_4) of the six carbon chain. This higher molecular mobility gradient itself may be accounted for by the rigidity induced by the glucopyranosyl cycle in maltitol. In the case of sorbitol, in the temperature range studied, the α and β relaxation processes are about to merge, and as a consequence, the mobility gradient between the C_1 and C_4 atoms is reduced.

5.3. The Role of Conformation Transitions

The microscopic picture that emerges from the simulations is discussed in this section. The analysis is focussed on the importance of conformational transitions in the dynamic processes. On the one hand, in both polyols, τ_1,

TABLE VIII Ratio τ_4/τ_1 of the relaxation times of the carbon atoms C_1 and C_4

T(K)	350	400	420	450	500
τ_4/τ_1 sorbitol	23	6	7	7.5	5
τ_4/τ_1 maltitol	–	17	26	7.5	5.9

the average time between two conformation transitions, $1/N_1$, and the torsional correlation time $\tau_{\phi 1}$ are of the same order of magnitude on the whole temperature range where they may be evaluated (Figs. 9 and 10). $1/N_1$ and $\tau_{\phi 1}$ can be accounted for by an Arrhenian behaviour, and the corresponding activation energy is very similar to the activation energy obtained from the relaxation time τ_1.

This rather good agreement should be considered with care in view of the low number of conformational transitions observed during the simulation runs. Yet, this result suggests that:

(i) in both polyols, the main contribution to the C_1—H vector reorientation is associated with local conformation transitions.
(ii) in both polyols, after the first few picoseconds, the overall rotational diffusion is dominated by conformation transitions.

In the case of the torsion angle a_3, the correlation time τ_4 is significantly lower than 1 ns (Figs. 6–7) above 500 K and 450 K, in maltitol and sorbitol respectively, and thus lower than the average time between two conformation transitions $1/N_3 > 1$ ns.

This result suggests that the conformational transitions are hindered in the middle of the molecule and that the C_3—H vector reorientation can not be accounted for only by conformational transitions. The overall rotational diffusion must be taken into account. At this point, it is worth commenting on the exponential functional form (Eq. (2)) used to fit the P_2 time decrease and mentioning the models that may account for this evolution [37–40]. In the framework of the Hall-Helfand or Monnerie *et al.*, models [38–40], if one neglects the librations motions and the correlated conformation transitions, corresponding to the smaller and larger time scales of the relaxation time spectrum respectively, the P_2 function obtained is a simple exponential:

$$P_2(t) = \exp(-t/\tau_0)$$

where the time scale τ_0 is characteristic of conformation transitions. As noted above, this simple exponential decrease is in good agreement with the results obtained from the molecular dynamics simulation. This suggests that one can separate two distinct time ranges to describe the relaxation process of sorbitol and maltitol. For short times, the relaxation process is especially the result of the librations. For longer times, the decrease of the correlation function can be interpreted as the effect of conformation transitions, and one can neglect in a first approximation any other mechanism that may have

a significant effect on the reorientation of the C—H vectors (librations and coupled conformation transitions). This simple picture can account for the C_1—H reorientation since we have found that τ_1 and $1/N_1$ are very similar. On the contrary, as mentioned above, the discrepancy between τ_4 and $1/N_3$ suggests that the use of the exponential functional form (Eq. (2)) may be a rather crude approximation and that additional motions like coupled librations, correlated conformations transitions or reorientation of longer segments of the molecule, may influence the C_4—H vectors reorientation.

6. CONCLUSION

In this paper, we have described molecular dynamics simulations of bulk sorbitol and maltitol together with ^{13}C NMR measurements of the correlation times of the carbon atoms of the main chain. We have examined the local dynamics common features and differences between the two polyols. The first conclusion that can be drawn from our study is the rather good agreement between the ^{13}C NMR results and the molecular dynamics simulations on bulk sorbitol and maltitol, on the basis of calculated P_2 correlation functions for the carbon atoms located at the end or in the middle of the chain. The relaxation times and the activation energy obtained compare well with the values derived from the NMR measurements. Moreover, the simulations give evidence of a lower mobility in maltitol. The simulations also supports the existence of a mobility gradient along the main chain, which is stronger in the case of the maltitol molecule. These mobility gradient may be intimately connected to the time scales shift between the α and β relaxation process. As a consequence, the higher gradient found in maltitol could be at the origin of the higher crossover temperature between the α and β relaxation processes in this polyol. On a chemical structure point of view, it could be the effect of the enhanced rigidity associated to the glucopyranosyl cycle. This conclusion about the connection between molecular motions of the carbons and the α and β relaxations must be careful in view of the small temperature range investigated. The motions of the carbon atoms at the end of the main chain are local processes which are not influenced by the cycle, and there is some evidence of a connection between the C—H vector reorientation and the conformational transitions in this case. Nevertheless, the molecular dynamics results indicates that more complex mechanisms should be taken into account in the case of the carbon atom in the middle of the chain.

References

[1] Murthy, S. S. N., Sobhanadri, J. and Gandasharan, G. (1994). "The origin of beta relaxation in organic glasses". *J. Chem. Phys.*, **100**, 4601.

[2] Flores, R. and Perez, J. (1995). "Mechanical spectroscopy of the beta relaxation in poly(vinyl chloride)". *Macromolecules*, **28**, 7171.

[3] Jho, J. Y. and Yee, A. F. (1991). "Secondary relaxation motion in Bisphenol A polycarbonate". *Macromolecules*, **24**, 1905.

[4] Spiess, H. W., Schmidt-Rohr, K. and Kulik, A. S. (1994). "Molecular nature of the β relaxation in poly(methyl methacrylate) investigated by multidimensional NMR". *Macromolecules*, **27**, 4733.

[5] Rigby, D. and Roe, R. J. (1987). "Molecular dynamics simulation of polymer liquid and glass. I. Glass transition". *J. Chem. Phys.*, **87**, 7285.

[6] Winkler, R. G., Ludovice, P. J., Yoon, D. Y. and Morawetz, H. J. (1991). "Computer simulations of n-alkane melts". *J. Chem. Phys.*, **95**, 4709.

[7] Fan, C. F. and Hsu, S. L. (1991). "Macromolecular simulation of amorphous polymers polysulfone". *Macromolecules*, **24**, 6244.

[8] Wagner, H. and Richert, R. (1999). "Equilibrium and non-equilibrium type β relaxations: D-sorbitol *versus* o-terphenyl". *J. Phys. Chem. B*, **103**, 4071.

[9] Olsen, N. B. (1998). "Scaling of the β relaxation in the equilibrium liquid state of sorbitol". *Journal of Non-Crystalline Solids*, **235–237**, 399.

[10] Nozaki, R., Suzuki, D., Ozawa, S. and Shiozaki, Y. (1998). "The α and β relaxation processes in supercooled sorbitol". *Journal of Non-Crystalline Solids*, **235–237**, 393.

[11] Faivre, A., Niquet, G., Maglione, M., Fornazero, J., Jal, J. F. and David, L. (1999). "Dynamics of sorbitol and maltitol over a wide time-temperature range". *Eur. Phys. J. B*, **10**, 277.

[12] Faivre, A., *Ph.D. Thesis*. "Etude des phénomènes de relaxation associés à la transition vitreuse". INSA-Lyon, 1997.

[13] Rössler, E., Hess, K. U. and Noviko, V. N. (1998). "Universal representation of viscosity in glass forming liquids". *J. Non. Cryst. Solids*, **223**, 207.

[14] Arbe, A., Richter, D., Comenero, J. and Farago, B. (1996). "Merging of the α and β relaxations in polybutadiene: a neutron spin echo and dielectric study". *Phys. Rev. E*, **54**, 3853.

[15] Johari, J. P. and Goldstein, M. (1970). "Viscous liquids and the glass transition.II. Secondary relaxations in glasses of rigid molecules". *J. Chem. Phys.*, **53**, 2372.

[16] Götze, W. and Sjögren, L. (1991). "Beta relaxation in supercooled liquids". *J. Non-Cryst. Solids*, **131–133**, 161.

[17] Margulies, M., Sixou, B., David, L., Vigier, G., Dolmazon, R. and Albrand, M. (2000). "Molecular mobility of sorbitol and maltitol: a ^{13}C NMR and molecular dynamics approach". *Eur. Phys. J. E*, **3**, 55.

[18] Eliel, E. L., Wilen, S. H. and Mander, L. N., Stereochemistry of Organic Compounds (John Wiley & Sons Inc., New York, 1994) pp. 11–13, 20–21.

[19] Hagler, A. T., Huler, E. and Lifson, S. (1974). "Energy functions for peptides and proteins. I. Derivation of a Consistent Force Field including the hydrogen bond from the amide crystals". *J. Am. Chem. Soc.*, **96**, 5319.

[20] Hagler, A. T. and Lifson, S. (1974). "Energy functions for peptides and proteins. II. The amide hydrogen bond and calculation of amide crystal properties". *J. Am. Chem. Soc.*, **96**, 5327.

[21] Lifson, S., Hagler, A. T. and Dauber, P. (1979). "Consistent Force Field Studies of intermolecular forces in hydrogen bonded crystals. I. Carboxylic acids, amides and the C=O...H—O hydrogen bonds". *J. Am. Chem. Soc.*, **101**, 5111.

[22] Hagler, A. T., Lifson, S. and Dauber, P. (1979). "Consistent Force Field Studies of Intermolecular fosrces in hydrogen bonded crystals. II. A benchmark for the objective comparison of alternative force fields". *J. Am. Chem. Soc.*, **101**, 5122.

[23] Hagler, A. T., Dauber, P. and Lifson, S. (1979). "Consistent force field studies of intermolecular forces in hydrogen bonded crystals. III. The C=O...H—O hydrogen bond and the analysis of the energetics and packing of carboxylic acids". *J. Am. Chem. Soc.*, **101**, 5131.

[24] Kitson, D. H. and Hagler, A. T. (1988). "Theoretical studies of the structure and molecular dynamics of a peptide crystal". *Biochemistry*, **27**, 5246.
[25] Andersen, H. C. (1980). "Molecular dynamics simulations at constant pressure and/or temperature". *J. Chem. Phys.*, **72**, 2384.
[26] Theodorou, D. N. and Suter, U. W. (1985). "Detailed molecular structure of a vinyl polymer glass". *Macromolecules*, **18**, 1467.
[27] Hutnik, M., Gentile, F. T., Ludovice, P. J., Suter, U. W. and Argon, A. S. (1991). "An atomistic model of the amorphous glassy polycarbonate of **4**,4'-isopropylidenephenol". *Macromolecules*, **24**, 5962.
[28] Li, Y. and Mattice, W. L. (1992). "Atom based modeling of 1,4-cis-polybutadiene". *Macromolecules*, **25**, 4942.
[29] Kim, E., Misra, S. and Mattice, W. L. (1993). "Atomistic models of amorphous polybutadienes 2. Poly(1-4-trans-butadiene), poly(1,2-butadiene) and a random copolymer of 1-4-trans-butadiene, 1-4-cis-butadiene and 1,2-butadiene". *Macromolecules*, **26**, 3424.
[30] Parrinello, M. and Rahman, A. (1981). "Polymorphic transitions in single crystals: a new molecular dynamics method". *J. Appl. Phys.*, **52**, 7182.
[31] Abragam, A., The principles of Nuclear Magnetism (Oxford University Press, London, 1961).
[32] Guillermo, A., Dupeyre, R. and Cohen Addad, J. P. (1990). "Homogeneity properties of NMR rates measured in molten polubutadiene. Temperature dependence of segmental chain motions". *Macromolcules*, **23**, 1291.
[33] Cohen Addad, J. P. (1993). "NMR and fractal properties of polymeric liquids and gels". *Prog. NMR Spectrosc.*, **25**, 1.
[34] Lartigue, C., Guillermo, A. and Cohen Addad, J. P. (1997). "Proton NMR investigation of the local dynamics of PEO in PEO/PMMA blends". *J. Polym. Sci. B: Polym. Phys.*, **35**, 1095.
[35] Fan, C. F., Cagin, T., Shi, W. and Smith, K. A. (1997). "Local chain dynamics of a model polycarbonate near glass transition temperature: a molecular dynamics simulation". *Macromol. Theory Simul.*, **6**, 83.
[36] Kim, E. G. and Mattice, W. L. (1994). "Local chain dynamics of bulk amorphous polybutadiennes: a molecular dynamics study". *J. Chem. Phys.*, **101**(7), 6242.
[37] Moe, N. E. and Ediger, M. D. (1995). "Molecular dynamics computer simulation of polyisoprene local dynamics in dilute toluene solution". *Macromolecules*, **28**, 2329.
[38] Hall, C. K. and Helfand, E. J. (1982). "Conformational state relaxation in polymers: time-correlation functions". *J. Chem. Phys.*, **77**, 3275.
[39] Valeur, B., Jarry, J. P., Geny, F. and Monnerie, L. (1975). "Dynamics of macromolecular chains. I. Theory of motions on a tetrahedral lattice". *J. Polym. Sci., Polym. Phys. Ed.*, **13**, 667.
[40] Dejean de la Batie, R., Lauprêtre, F. and Monnerie, L. (1988). "Carbon-13 NMR investigation of local dynamics in bulk polymers at temperatures well above the glass-transition temperature. 3-cis-l,4-poly(butadiene) and cis-l,4-polyisoprene". *Macromolecules*, **21**, 2045.